Computational optimization of $CH_4/H_2/CO$ blends in a spark-ignition engine using quasi-dimensional combustion model

Amin Paykani[a,*], Christos E. Frouzakis[b], Christian Schürch[b], Federico Perini[c], Konstantinos Boulouchos[b]

[a]*School of Physics, Engineering and Computer Science,University of Hertfordshire, Hatfield, UK*
[b]*Aerothermochemistry and Combustion Systems Laboratory, Swiss Federal Institute of Technology Zurich, CH-8092 Zurich, Switzerland*
[c]*Wisconsin Engine Research Consultants LLC, Madison, WI, USA*

Abstract

Recent research has proven that computational fluid dynamics (CFD) modeling in combination with a genetic algorithm (GA) algorithm is an effective methodology to optimize the design of internal combustion (IC) engines. However, this approach is time consuming, which limits the practical application of it. This study addresses this issue by using a quasi-dimensional (QD) model in combination with a GA to find optimal fuel composition in a spark ignition (SI) engine operated with $CH_4/H_2/CO$ fuel blends. The QD model for the simulation of combustion of the fuel blends coupled with a chemical kinetics tool for ignition chemistry was validated with respect to measured pressure traces and NO_x emissions of a small size single-cylinder SI engine operated with CH_4/H_2 blends. Calibration was carried out to assess the predictive capability of the QD model, and the effect of hydrogen addition on the lean limit extension of the methane fueled engine was studied. A GA approach was then used to optimize the blend composition and engine input parameters based on a fitness function. The QD-GA methodology was implemented to simultaneously investigate the effects of three input parameters, i.e., fuel composition, air-fuel equivalence ratio and spark timing on NO_x emissions and indicated thermal efficiency (ITE) for the engine. The results found indicated that this approach could provide optimal fuel blends and operating conditions with considerable lower NO_x emissions together with improved thermal efficiencies compared to the methane fueled engine. The presented computationally-efficient methodology can also be used for other fuel blends and engine configurations.

Keywords:
SI engine; fuel composition; quasi-dimensional model; efficiency; GA optimization

---

*Corresponding author
Email address: a.paykani@herts.ac.uk (Amin Paykani)

Nomenclature

η	molecular viscosity [mP]	
λ	air-fuel equivalence ratio	
τ	time constant [s]	
θ	engine crank angle [CA]	
A	area [m^2]	
C	constant [–]	
D_3	fractal dimension of a 3D rough surface	
K_st	flame stretch factor	
L_I	integral scale of turbulence [m]	
L_T	Taylor's micro-scale of turbulence [m]	
m	mass [kg]	
n	engine rotating speed [rpm]	
Q	heat [J]	
r_k	initial flame kernel radius [m]	
s	engine stroke [m]	
S_L	laminar flame speed [m/s]	
t	time [s]	
u	velocity [m/s]	
ATDC	after top dead center	
BTDC	before top dead center	
CAD	crank angle degree	
CCV	cycle-to-cycle variation	
EGR	exhuast gas recirculation	
EVO	exhaust valve opening	
GA	genetic algorithm	
ITE	indicated thermal efficiency	
IVC	inlet valve closing	
KI	knock integral	
LES	Large Eddy Simulation	
MFB50	crank angle at which 50% of the fuel mass fraction has burned	
NG	natural gas	
ON	octane number	

2

70	QD	quasi dimensional
71	RANS	Reynolds-averaged Navier–Stokes
72	RMSE	root mean square error
73	SA	spark advance [CAD]
74	SI	spark ignition [CAD]

1. Introduction

The passenger cars, motorcycles and small engines rely on Spark Ignition (SI) combustion mode, but because of the low compression ratio and stoichiometric operation, their thermal efficiency is limited. Increasing per capita energy demand and stringent CO_2 emissions regulations motivate the use of low-carbon fuels in the transport sector. Natural gas has a crucial impact on reducing CO_2 emissions from combustion engines thanks to their favorable H/C ratio [1]. Additionally, the high octane number and high knock resistance of methane allows to run the engine on higher compression ratios [2, 3]. Moreover, lean natural gas combustion has shown the potential to improve efficiency compared to stoichiometric gasoline engines, but suffers from unstable and poor ignitability of the fuel-air mixture, leading to incomplete combustion or misfire [4]. The reduction of flame speed at lean operation results in significant cycle-to-cycle variations (CCV) [5]. Hydrogen is considered a suitable candidate as additive for lean-burn natural gas fueled SI engines, due to its higher laminar flame speed, wider flammability limits and small quenching distance [6, 7].

Syngas derived from natural gas, coal, biomass, or hydrocarbon feedstock, is primarily consisted of hydrogen and carbon monoxide, which has also been considered as a future fuel for internal combustion (IC) engines, since in addition to offering similar advantages as hydrogen it can also be produced on-board through fuel reforming [8, 9]. Fuel reforming has been shown to be an effective method to add syngas to the intake charge for lean and dilute SI operation [10]. Syngas operated SI engine is expected to reduce the lean misfire limit, which decreases the flame development duration leading to improved engine lean burn capability. However, syngas also affects the engine volumetric efficiency, and typically has a lower heating value compared to liquid fuels [11]. Considerable power output derating (20%-30%) has been reported for direct use of syngas in engines designed for natural gas operation [12]. Addition of natural gas into syngas to form a fuel blend is an effective method to minimize power derating and increase thermal efficiency of the engine [13]. In addition, NO_x emissions can benefit from syngas combustion because of lean operation.

Trial and error approaches have been extensively used to study methane-syngas fuel blends in SI engines [14–18]. However, the optimal composition of the fuel blend can be determined numerically to satisfy the requirements of improved performance and low exhaust emissions, in order to prevent costly experiments. In a first step towards using optimization to determine computationally

the optimal composition of gaseous fuels in SI engines, Paykani et al. [19] employed simple models to study how ignition delay times and high laminar flame speeds can be optimized by adding hydrogen and syngas to methane to obtain optimal fuel blends under engine-relevant conditions.

Currently, 3-D engine simulations are being extensively used for the IC engine research, however, optimization of complex engine configurations relies mainly on computationally efficient simulation tools, such as zero-dimensional (0D) and quasi-dimensional (QD) models, since extensive experimental investigations can be costly and time-consuming (see, for example, [20]). There are several research works in the literature where a QD model was employed for combustion modeling in SI engines, but a few have considered fuel blends with a wide blending range and operating conditions (e.g. [21, 22]). The main challenge in using QD model for fuel blend stems from variations in laminar flame speed.

The aim of this paper is to bridge the gap by developing a computationally cost-effective numerical tool for optimizaiton of the fuel blend and combustion system in an SI engine. A QD combustion model was presented and validated through experiments in a small, single-cylinder SI engine.The QD combustion model proposed here builds upon the previous models and includes an extension of the QD model developed in an earlier work of Perini et al. [23]. Then a genetic algorithm (GA) optimization methodology was coupled to the QD model to simultaneously optimize fuel blend composition and engine input parameters of the SI engine. Major novelties of the present methodology include the extensive work on fuel blends and optimization, as well as validations in a SI engine for a wide range of operating conditions. The computational study demonstrates the applicability of a rigorous but computationally cost-effective numerical optimization strategy for SI engines operating with gaseous fuel blends.

2. Engine specifications and experimental facility

A series of measurements were carried out on a Swissauto Wenko 250 cm^3 four-stroke single cylinder SI engine on a test bench shown schematically in Fig. 1. The engine specifications are given in Table 1. In order to calculate the output torque and control the speed, the engine is mounted on a water-cooled eddy current dyno. A gas mixing system consisting of one flow sensor for CH_4 and three flow controls for the other gases is mounted before the gas valve in order to change the desired fuel mixture of CH_4 and H_2. For this study, no synthetic exhaust gas recirculation (EGR) has been taken into account. For correct model parameter calibration, a venturi mixer homogeneously mixes the intake air and the fuel until it reaches the engine.

3. Numerical methodology

In the following sections the submodels used in this study will be explained. First, the laminar flame speed calculation for fuel blends is presented which is an important part of the QD combustion model.

4

Table 1: Engine Specifications.

Engine name	Swissauto
Number of cylinders	1
Bore (mm)	75
Stroke (mm)	56.5
Connecting rod length (mm)	95
Total displacement (cc)	250
Compression ratio	12.5:1
IVC (CA deg ATDC)	-112
EVO (CA deg ATDC)	109
Fuel supply	Venturi gas mixer, naturally aspirated
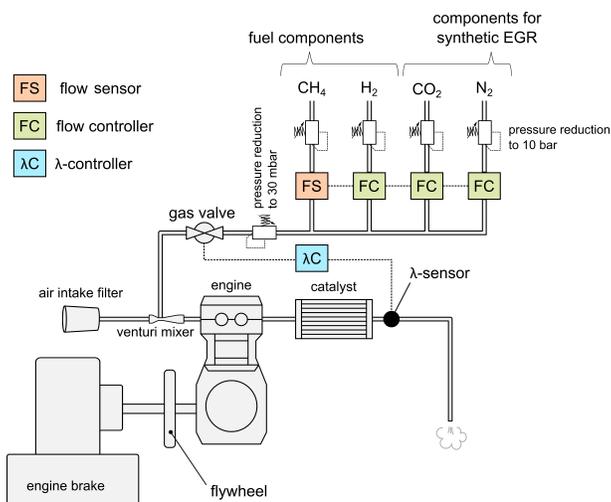
Figure 1: The engine test facility allows for freely adjustable CH_4/H_2 fuel mixtures and operation with synthetic EGR.

3.1. Laminar flame speeds

Laminar flame speed calculations for the CH_4/H_2 and $CH_4/H_2/CO$ blends have been discussed in our recent published paper [19]. Since no suitable correlation for laminar flame speed was found in the literature for engine-relevant conditions, reaction kinetics computations were used to tabulate the flame speeds. In particular, a lookup table for S_L as a function of fuel composition, temperature, pressure, and equivalence ratio was generated using Cantera [24] within the ranges listed in Table 2. Following a comparative study of ignition delay times and laminar flame speeds of methane-based fuel blends under engine-relevant conditions with experimental data, the 290Rxn mechanism [25] was selected and is also employed in the present study. It is a reduced version of AramcoMech1.3 mechanism [26] containing 72 species and 290 reactions, and has been successfully used to predict the ignition properties of biogas and syngas fuel mixtures,

5

as well as natural gas [25].

Table 2: Ranges of tabulated conditions for the laminar flame speed.

Parameter	Range	Step size
Pressure	$5 - 95$ bar	15 bar
Temperature	$280 - 1000$ K	120 K
Air-fuel equivalence ratio (λ)	$1.0 - 1.8$	0.16
H_2/syngas fraction	$0.0 - 0.5$	0.125

3.2. Quasi-dimensional combustion model

A two-zone, quasi-dimensional (QD) model for the simulation of combustion with methane-based fuel blends SI engine is presented. In QD models, the mass burning rate is computed by a predictive expression and the geometrical parameters are characterized in the form of a thin flame front interface separating burned from the unburned gases [20]. The two-zone thermodynamic model has been already used in different papers (e.g. [27, 28]), and the detailed description can be found in [23, 29, 30].

Accurate submodels are critical for the predictive capability of a QD model, particularly the ones for ignition, combustion, heat transfer and knock, and a submodel was used for the prediction of NO_x emissions, as described in the following subsections.

3.2.1. Ignition model

Simple models are typically used to model ignition in SI engines. The initial flame kernel is often considered as a certain mass or volume [29]. In this work, an initial flame kernel with a constant volume is assumed. Although such an initialization is arbitrary, it has provided acceptable results in previous works [23, 31]. The kernel shape was selected to be sphere with radius of $r_k = 0.01$ m. Sensitivity analysis of maximum in-cylinder pressure and crank angle degree in ignition kernel modeling was also performed around this value with 10% change and the results were reported in the Fig. 2. The sensitivity analysis of flame kernel was done to define the sensitivity of the model with respect to this constant in different operating condition and find out which case number is more sensitive to the flame kernel size. The kernel shape was selected to be sphere with radius of $r_k = 0.01$ m. Generally the value of the kernel size should be chosen in a way that the model results capture the experimental data.

3.2.2. Combustion model

The fractal combustion model based was employed, where the entrainment of unburned gas into the mean flame front was modeled by Blizzard and Keck [32] as,

$$\frac{dm_e}{dt} = \rho_u \, A_f \, u_{te} \tag{1}$$

6
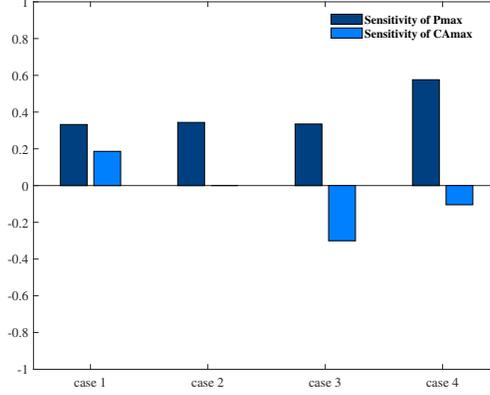
Figure 2: Sensitivity of the maximum in-cylinder pressure and crank angle degree in ignition kernel modeling.

Here, u_{te} is the 'turbulent entrainment' velocity, and A_f denotes the mean flame front area. The accurate flame front area prediction is important for the mass fraction burned profiles. The mass burning rate can be assumed to be proportional to the unburned mixture's mass within the entrainment front,

$$\frac{dm_b}{dt} = \frac{m_e - m_b}{\tau_b}, \qquad \tau_b = C_{\tau_b} \frac{L_T}{S_L} \tag{2}$$

A characteristic time constant τ_b is used to control this process, which is calculated as the ratio of the Taylor micro-scale length to the laminar burning velocity.

The fractal-based methodology has been widely showed good results for combustion modeling of SI engines [33–35]. A better agreement with the experimental results, a better replication of the overall burn rate shape, and a reduced tuning effort have been demonstrated compared to the eddy burn-up theory [36]. The model assumes that flame wrinkling dominates the burning rate and the wrinkled surface area of the flame can be characterized by a fractal geometry [37]. Turbulence causes the flame wrinkling, hence increases its surface area and consequently the flame speed

$$u_t = u_L \left(\frac{L_{\max}}{L_{\min}}\right)^{D_3 - 2} \tag{3}$$

where u_L is the laminar burning velocity of the stretched flame front, L_{min}, L_{max} denote the minimum and maximum turbulence wrinkling scales, respectively, and D_3 is the fractal dimension of a three-dimensional rough surface. Matthews and Chin [38] proposed the following stretch model for the relationship between S_L and u_L

$$u_L = S_L(1 - \frac{\eta_u}{\rho_u S_L{}^2} K_{st}) \tag{4}$$

7

in which η_u is the molecular viscosity of the unburned mixture, and K_{st} the flame stretch factor [39]. Santavicca et al. [40] introduced a reliable expression for the prediction of D_3 as

$$D_3 = C_{D_3} 2.35 \frac{u'}{u' + S_L} + 2.0 \frac{S_L}{u' + S_L} \tag{5}$$

For suitable in-cylinder turbulence modeling, a simple turbulence model, first proposed by Hall and Bracco [41] was considered

$$u'_{TDC} = 0.75\bar{u}_p = 0.75(2sn), \quad u' = C_{u'} u'_{TDC}(1 - \frac{\theta}{90}) \tag{6}$$

Finally, the transient flame development phase from early flame kernel growth to fully developed turbulent flame for the accurate prediction of turbulent burning velocity was considered based on the ratio suggested by Lipatnikov and Chomiak [42]

$$\frac{u_{t,t}}{u_t} = \left\{ 1 + \frac{\tau'}{t} \left[\exp\left(-\frac{t}{\tau'} - 1 \right) \right] \right\}^{1/2}, \qquad \tau' = 0.55 C_{\tau'} L_I / u' \tag{7}$$

The turbulent burning velocity calculated from Eq. (3), and corrected with the exponential term for its transient development (Eq. (7)) gives the turbulent entrainment velocity u_{te} in Eq. (1), and thereby closes the model of turbulent flame development and combustion. The expressions for the fractal-based combustion model are shown in Fig. 3.

3.2.3. Wall heat transfer

A combined convective and radiative heat transfer approach was employed. The methodology couples a convective heat transfer coefficient according to [43] to a radiative term [44], for considering high temperature burned gases effects,

$$\frac{dQ}{dt} = C_Q \left(\frac{dQ_{h_0}}{dt} + \frac{dQ_r}{dt} \right) \tag{8}$$

where C_Q is a calibration coefficient. In addition, wall heat losses are distributed according to the wall-wetting area at the two zones.

3.2.4. Knock model

Variations of fuel composition in gas-fueled IC engines can lead to engine knock as a result of autoignition in the unburnt zone during the regular combustion process [45]. Autoignition depends on reactivity of the fuel-air diluted mixture in the end gas, and is usually characterized by the autoignition delay time [46]. Knock modeling in SI engines ranges from simple empirical expressions to complex formulations featuring chemical kinetics [47–49]. The Livengood integral [50] (Eq. (9) below) is widely used in knock models for 0D/1D-simulations as it is a fast and easy to calibrate method for estimating the onset of autoignition and consequently the onset of knock.
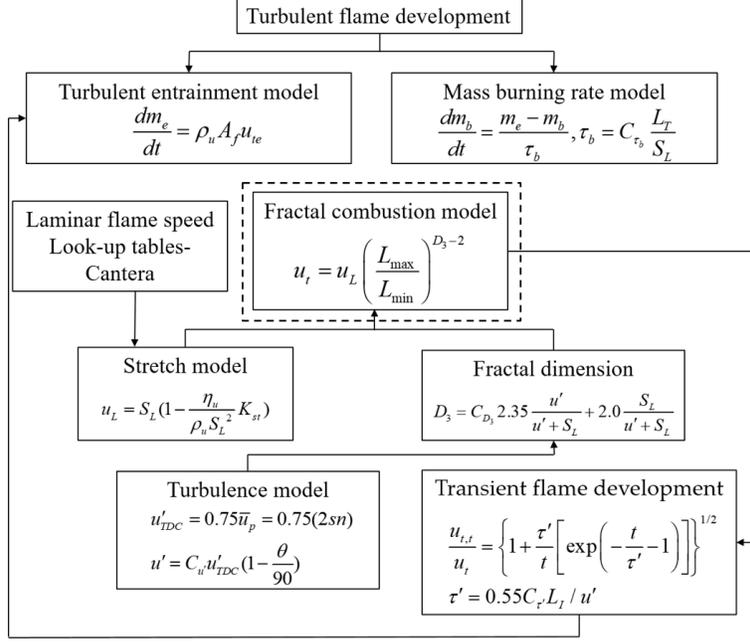
Figure 3: The fractal-based combustion model.

The knock integral (KI) has been used to describe a state related to a critical hypothetical indicator for the progress of the autoignition process of the end gas. By integrating its instantaneous value during the compression and combustion strokes, the overall ignition delay time can be computed, and is specified when the knock integral reaches the value of one,

$$\int_{t_{IVC}}^{t_{KO}} \frac{dt}{\tau(t)} = 1 \qquad (9)$$

Here, t_{IVC} and t_{KO} are the times at intake valve closure and knock onset, respectively, and $\tau(t)$ is the instantaneous autoignition delay time. For the autoignition delay time calculation, a simple Arrhenius correlation is used for knock modeling [45]

$$\tau = A p^n e^{\frac{B}{T}} \qquad (10)$$

A, n and B are mixture-dependent parameters. For QD engine models, empirical expressions have been shown to yield good results [47]. Several well known parameter sets for Eq. (10) were tested in this study, and the most widely used one based on recording the knock onset in a CFR engine for various operating conditions [51] was selected

$$A = 0.01869 \left(\frac{ON}{100}\right)^{3.4017}, \quad n = -1.7, \quad B = 3800 \qquad (11)$$

9

3.2.5. NO$_x$ emissions

The minimization of NO$_x$ emissions from SI engines is a crucial design target, and the QD combustion simulation framework must include a submodel for NO$_x$ emissions. The main source mechanism (thermal-NO) is considered here, while 'prompt' NO, which describes the formation of NO at the flame fronts was neglected. The extended Zel'dovich mechanism listed in (Table 3) [52] was employed in the simulations, and the reaction rate expression for NO is modified by the introduction of a calibration coefficient c_{NO}, which multiplies the forward reaction rate of the first reaction

$$r_{NO} = c_{NO}k_{f,1}[N_2][O] - k_{b,1}[NO][N] + k_{f,2}[N][O_2] - k_{b,2}[NO][O] + \\ k_{f,3}[N][OH] - k_{b,3}[NO][H] \tag{12}$$

Table 3: Arrhenius coefficients for the forward reactions of the extended Zel'dovich mechanism [23].

Reaction	A	b	E (kJ/kmol)
$N_2 + O \rightleftharpoons NO + N$	3.30×10^{12}	0.20	0.0
$N + O_2 \rightleftharpoons NO + O$	6.40×10^{9}	1.00	3160.0
$N + OH \rightleftharpoons NO + H$	3.80×10^{13}	0.00	0.0

4. Model calibration

The model was calibrated over the wide range of experimentally studied engine operating conditions summarized in Table 4. The measurement matrix comprises variable methane-hydrogen ratio, air-fuel equivalence ratio and spark timing at a constant engine speed of 3000 rpm and fully unthrottled operation.

Table 4: Validation cases and operating parameters.

Case	Speed (rpm)	λ (-)	f$_{H_2}$ (%vol)	Spark timing (ST) (CA BTDC)
1	3000	1.4	0	45
2	3000	1.4	10	45
3	3000	1.4	25	45
4	3000	1.4	25	60
5	3000	1.6	10	45
6	3000	1.6	25	45
7	3000	1.6	50	45
8	3000	1.6	25	70
9	3000	1.8	50	45
10	3000	1.8	50	60
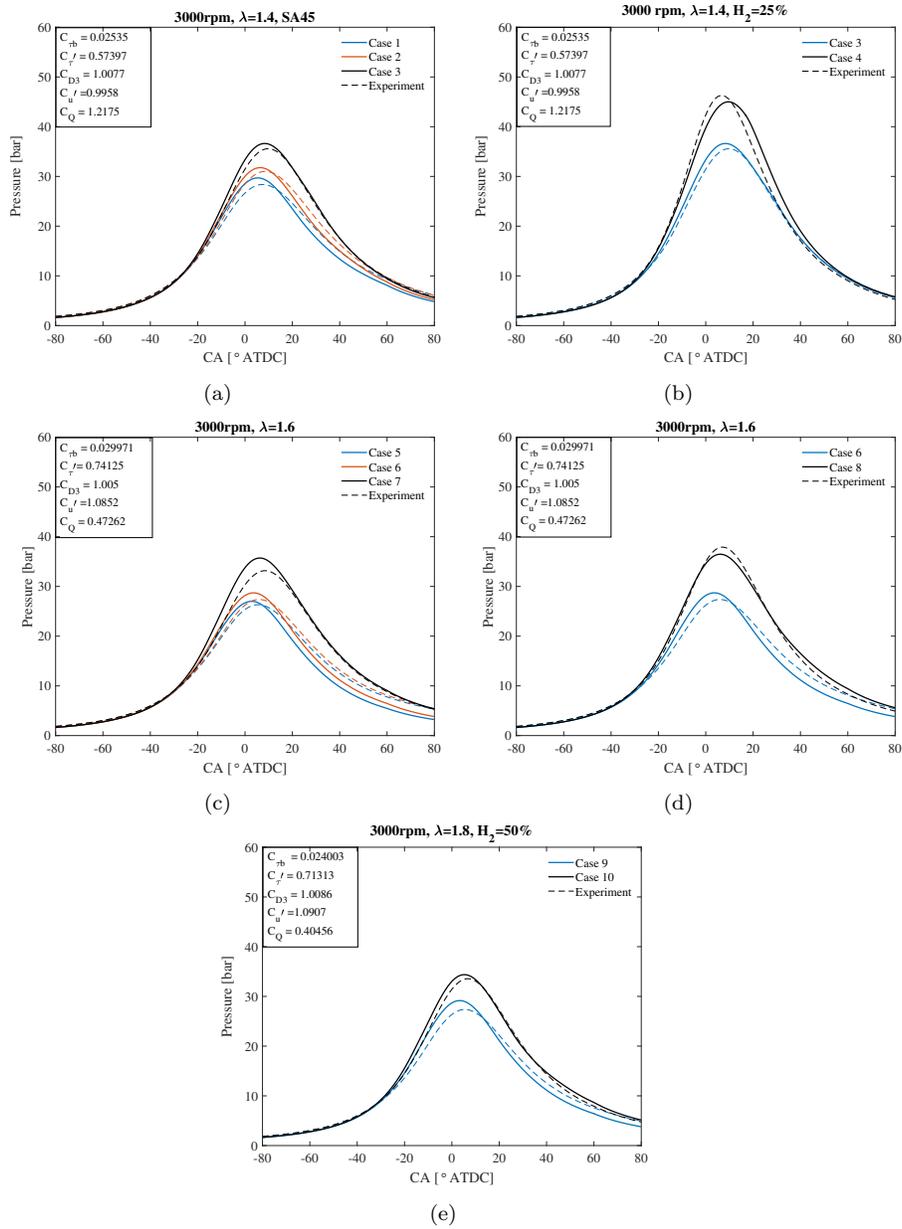
Figure 4: Comparison of the measured (dashed lines) and the computed (solid lines) in-cylinder pressure validation for the calibration constants specified for different cases.

4.1. Model calibration

The model was calibrated on the set of five coefficients regarding flame development, turbulence–flame interaction and heat transfer submodels: C_Q for heat transfer modeling, C_{D_3} for the fractal dimension of the developed flame front surface, the $C_{u'}$ multiplier of the in-cylinder rms turbulence, $C_{\tau'}$ for transient turbulent flame development, and C_{τ_b} which is used for estimating the overall burning rate time. For the optimization study, we need a specific set of coefficients, which can yield good in-cylinder pressure predictions for the desired range of the operating conditions. Since it is unlikely to obtain a set of specific coefficients for all the studied cases in Table 4, validation and calibration focused on three air-fuel equivalence ratios $\lambda = 1.4, 1.6, 1.8$. The coefficients were calibrated using simultaneous multi-objective minimization of the root mean square error (RMSE) between measured and calculated in-cylinder pressure traces by means of GA. Simulations were performed with values for all five coefficients varying within a specified range, and the results at the ten operating conditions of Table 4 are compared to the experimental in-cylinder pressure traces and NO_x emissions in Figs. 4 and 5, respectively, showing a good agreement with low RMSE error for all ten cases.

By operating the engine at hydrogen enriched methane of up to 50%/50% CH_4/H_2, it can be seen that the combustion process becomes faster, due to the higher flame speed of the blend. From the emissions point of view, higher hydrogen content generally results in increased NO_x emissions, although by moving to a leaner point these can be lowered while still maintaining a similar efficiency [53]. It is evident that for the leanest case of $\lambda = 1.8$, NO_x emissions are almost negligible.

5. Genetic algorithm optimization strategy

A genetic algorithm (GA) was used to optimize the model output for the input parameters listed in Table 5 together with their respective ranges of variation selected on the basis of the available experimental data and consideration of the knock limit. Fuel composition and spark timing are design parameters at different air-fuel ratio λ. The ranges of variation included the baseline condition with pure methane operation. A properly-defined merit function is vital to the efficiency and success of a GA. In this study, the following merit function is used based on the work of Montgomery [54]

$$Merit = \frac{1000}{NO_x/NO_{x\_Base} + ITE_{Base}/ITE} \qquad (13)$$

where ITE_{Base} and NO_{x_Base} are the indicated thermal efficiency and NO_x emissions for the pure methane (case 1 in Table 4), respectively. The goal is to demonstrate how the optimal results would improve ITE and NO_x emissions compared to the base case (methane fueled engine). The optimization study was performed based on the calibration, optimal parameters were obtained at specific λ and finally the best case was selected.

(a)   (b)

(c)
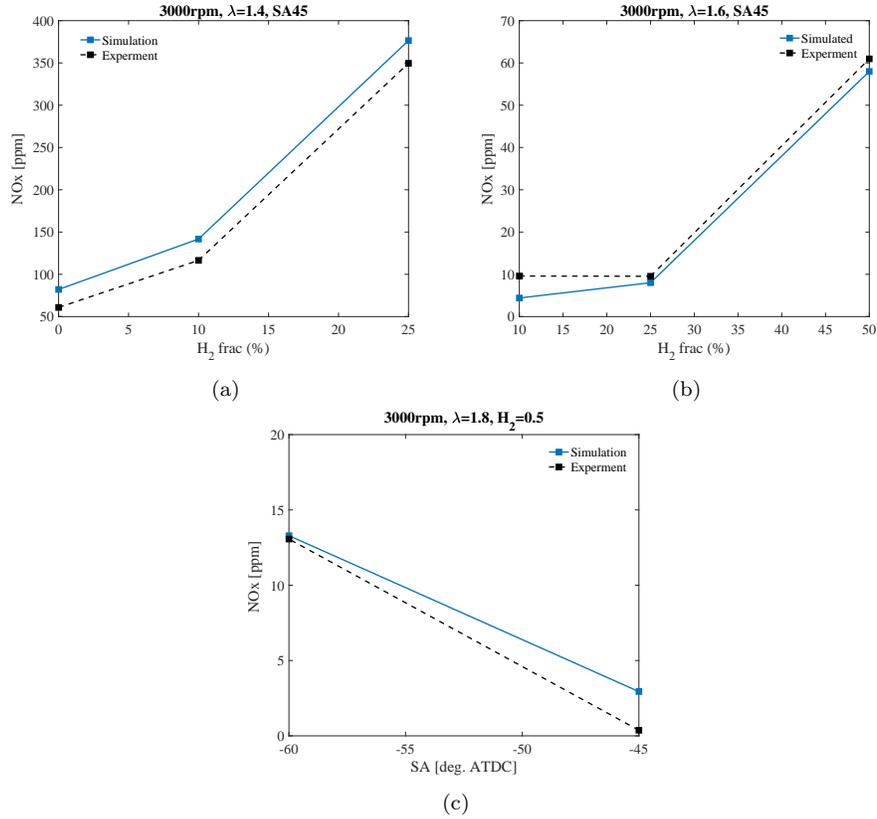
Figure 5: Comparison of the measured (dashed lines) and computed (solid lines) NO_x emission.

Table 5: GA design parameters and ranges.

Parameter	Range
H_2/syngas (%vol)	$0 - 50$
Air-fuel equivalence ratio (λ)	$1.4 - 1.8$
Spark advance (^oCA BTDC)	$10 - 80$

5.1. QD-GA approach

The flowchart of the QD-GA methodology is illustrated in Fig. 6. A GA takes a "survival of the fittest" approach to optimize a design, and was run with a population of 20 individuals for 20 generations until the merit function converged, i.e., reached a maximum value globally. Each individual is a QD simulation case with a set of input parameters, which were initialized randomly, and each subsequent generation consists of a population containing the best individual from the previous generation. The merit values for the individuals were

13

Start

Initialize

Max Generation Number (Stop Criterion)

Yes — **Stop the iteration**

Report Optimum solution

No — **Apply Crossover and Mutation Operators**

Merge All Populations Created from Previous generation (or initial Population in 1st generation) , Crossover and Mutation Operators

Positions

Sort Populations Based on the Costs

Costs

Replace Populations with Previous Populations and Keep best individuals

Combustion model: Quasi dimensional model with considering turbulence effect on flame geometry and speed

Constant volume kernel, adiabatic temperature

Post flame zone (flame products, equilibrium calcs., Cantera), Tb, Mb, Vb Thermodynamic properties (Cp, R, ...), Cantera

Turbulence effect using a fractal based model

Laminar flame speed, Cantera, Look-up table

Unburned zone (air, fuel) Tu, Mu, Vu Thermodynamic properties (Cp, R, ...), Cantera

Combined Hohenberg convective and radiative heat loss

Figure 6: Flowchart of QD-GA solution methodology.

evaluated after each generation was completed and the population was monitored for similarity between the individuals. Convergence was achieved when the the maximum merit value was reached. The evolution of the merit function towards its maximum value during the progress of the QD-GA optimization for a sample case is shown in Fig. 7.

6. Results and discussion

In this section, results from the QD modeling and the QD-GA approach for the fuel blends are presented and discussed. The outputs of the optimized configurations are compared against the baseline case as well as the QD results.

6.1. QD modeling results

The effect of H_2 fraction and spark timing variations on the indicated thermal efficiency ITE, maximum pressure, MFB50 and NO_x emissions at λ=1.4 are shown in Fig. 8. The ITE and maximum pressure is found to increase by H_2 addition and spark timing advance. As seen in Fig. 8, at higher hydrogen fractions and spark advance (SA) timings, MFB50 is advanced resulting in higher maximum pressures and ITE values. This has an adverse affect on NO_x emissions which are found to increase considerably by advancing the spark timings from -50 to -80 CAD ATDC and increasing the hydrogen from 15 vol% to 50

14
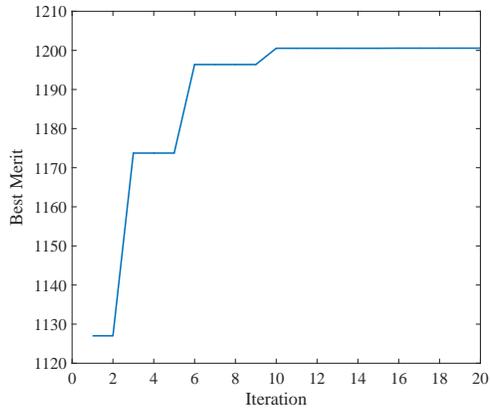
Figure 7: Evolution of the merit function using the QD-GA approach for methane-hydrogen blend at λ =1.8.

vol%. Hydrogen addition increases flame speed and shortens the combustion duration, resulting in higher in-cylinder temperatures and pressures, which promote NO_x formation. The best way to lower the NO_x emissions is to increase λ and/or retard the spark timing leading to lower mixture temperatures and reduced residual time of air in the heated zone. It can be concluded that in order to meet the requirement of high thermal efficiency and lower NO_x emissions lower H_2 fraction and spark advance timing in the range of -30 to -50 CAD ATDC would be the optimal choices to avoid knock propensity, high NO_x emissions and misfiring for the studied engine.

The effect of hydrogen content and spark timing on knock onset and knock integral in the methane-fueled engine at λ=1.4 are shown in Fig. 9.

It can be seen that with advanced spark timing the knock integral increases. It is also evident that knock appears at H_2 content higher than > 25% with excessive spark timing advancing. Increased knock with higher H_2 fractions is due to the higher autoignition propensity and the wider flammability limit of hydrogen, while methane has higher knock resistance because of its higher ignition delay time. Detailes of autoignition delay times and laminar flame speeds for methane, methane/hydrogen and methane/syngas blends have been discussed in our previous paper [19]. Hydrogen addition increases the burning velocity and reduces the heat capacity of the blend leading to significantly higher end-gas temperature and pressure [55]. Hydrogen also has a very short flame quenching distance compared to methane, which allows flames to travel closer to the cylinder walls and results in the more severe knocking characteristics of higher H_2 content blends.
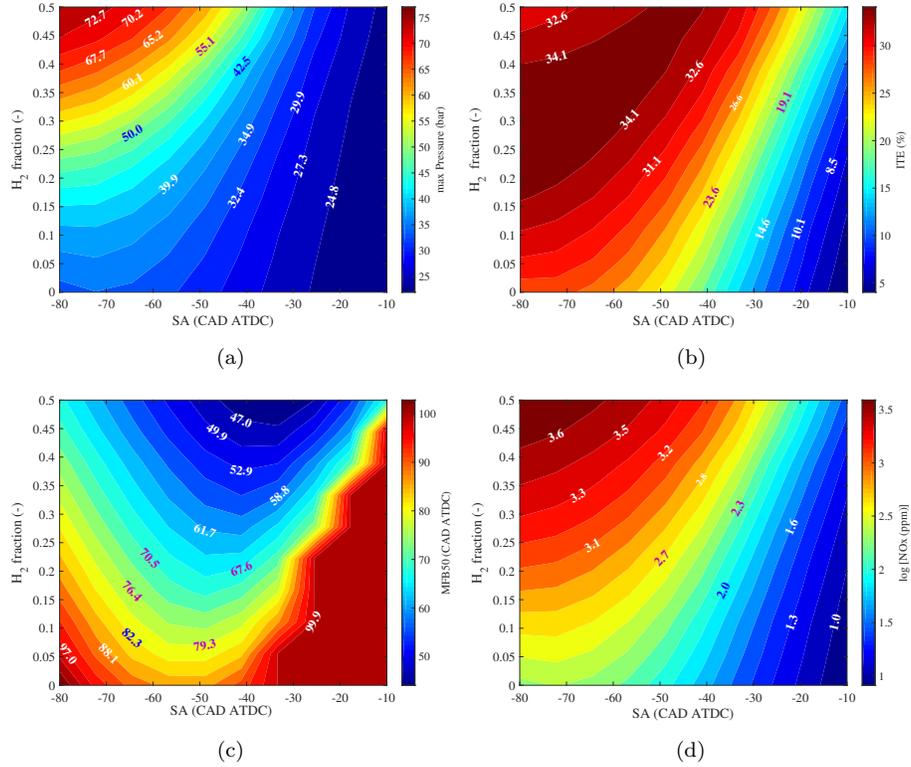
Figure 8: Effects of hydrogen content and spark timing on ITE and NO_x emissions for methane fueled engine at λ=1.4; (a) maximum pressure, (b) ITE, (c) MFB50, (d) NO_x emissions.

6.2. Optimization results

6.2.1. Methane/hydrogen blend

The composition of methane/hydrogen blends and spark timing were optimized for the SI engine operating conditions at three λ values. Figure 10 presents ITE versus NO_x emissions points for this optimization study obtained from simulations, in which the base and optimal cases found by the algorithm are highlighted. It was found that the ITE-NO_x trade-off is in agreement with the parametric study results of Ma et al. [53]. The trade-off extends towards higher ITEs and lower NO_x emissions as the λ increases. The temporal evolution of in-cylinder pressure for both base and optimal cases are shown in Fig. 11. It is noteworthy that at $\lambda = 1.4$ the base and optimal cases are identical and it can be inferred that for quite lean mixtures, hydrogen addition is not effective in terms of NO_x emissions. For ultra-lean conditions, due to the hydrogen content in the blend and advanced spark timing the pressure is higher in the optimal case found by the algorithm. Thus, the total work done in the optimal case is
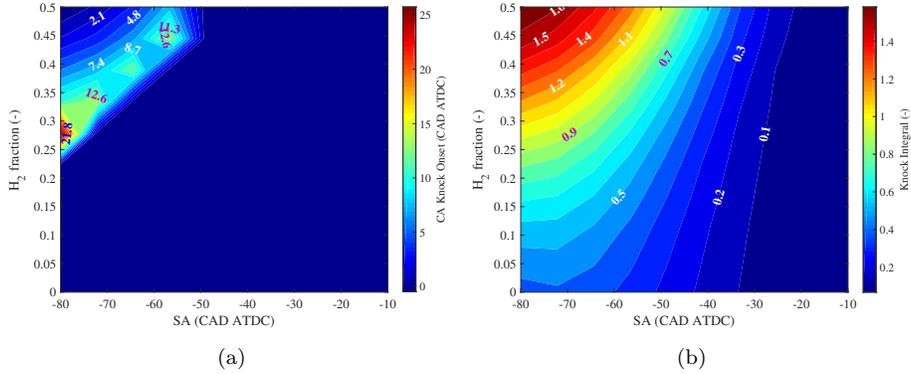
Figure 9: Effects of hydrogen content and spark timing on knocking in methane fueled engine; (a) knock onset; (b) knock integral.

higher with appropriate combustion phasing, resulting in higher ITEs and lower NO_x emissions.

From the chemical kinetics point of view, increased concentrations of OH, O and H radicals can be found with hydrogen addition to methane resulting in reduced ignition delay times and enhanced laminar flame speeds of CH_4/H_2 blends [56, 57]. Hydrogen addition increases combustion efficiency due to shorter burn duration, which is beneficial for the engine to operate at higher λ values. However, at constant λ, hydrogen addition leads to higher peak in-cylinder pressures as a result of shorter burn duration.

The increased laminar flame speed obtained from addition of hydrogen results in faster combustion and therefore higher temperatures inside the cylinder, which leads to higher NO_x emissions at constant λ.

It should be noted that when λ is increased to 1.8, hydrogen fraction and spark timing shifts toward higher values in the optimal case found by the algorithm. It was found that ultra-lean combustion can compensate the demerits of advanced spark timing and high hydrogen contents in terms of NO_x emissions, which are lower in the optimal case found by the algorithm because of the lower combustion temperatures associated with ultra-lean mixtures despite hydrogen addition.

The input parameters and the corresponding outputs for both the base case (case 1 in Table 4) and the optimal case from all simulations are listed in Table 6. The optimal case found by QD-GA yielded higher indicated thermal efficiencies and reduced NO_x emissions over the base case of pure methane due to extending the lean limit of the engine. It can be seen that the optimal case corresponds to the $58.9\%CH_4/41.1\%H_2$, λ=1.8 and SA = 80 CAD BTDC.

6.2.2. Methane/syngas blend

The same approach was used to obtain the optimal composition for the methane and syngas blend for a mixture of $50\%H_2$-$50\%CO$ by volume. Figure 12

17
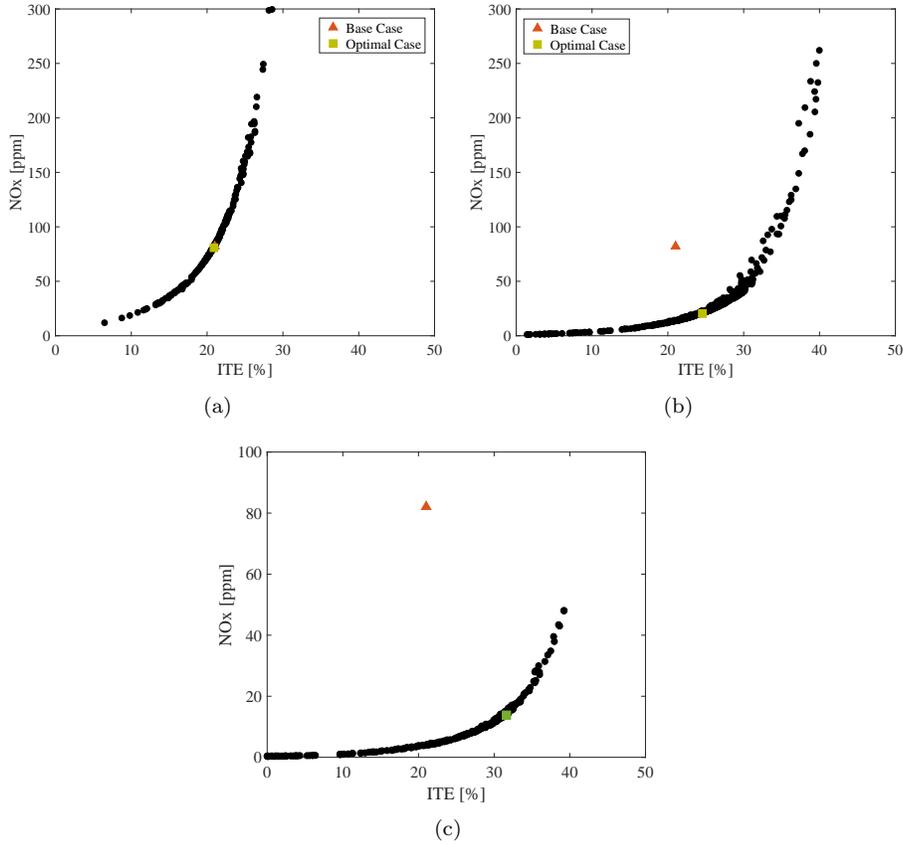
Figure 10: ITE versus NO$_x$ emissions for methane-hydrogen case including the base and optimum: (a) λ=1.4; (b) λ=1.6; (c) λ=1.8.

reports ITE versus NO$_x$ emissions points containing base and optimal cases for this optimization study. The same trend as in the methane/hydrogen case is noticed. The temporal evolution of in-cylinder pressure for both the base and optimal cases are depicted in Fig. 13. The addition of syngas to CH$_4$ accelerates combustion resulting in higher temperatures.

Not only H$_2$ but also CO can improve in-cylinder combustion and increase thermal efficiency. With the addition of syngas, the peak in-cylinder pressure increases, and flame development duration decreases compared to the pure methane case [58].

Syngas addition also tends to increase the NO$_x$ emissions due to the increased in-cylinder temperature.

The impact of syngas addition is slightly weaker than that of H$_2$ addition, but much stronger than that with addition of pure CO [19]. The NO$_x$ emissions are lower in the optimal case found by the algorithm because of the lower combustion
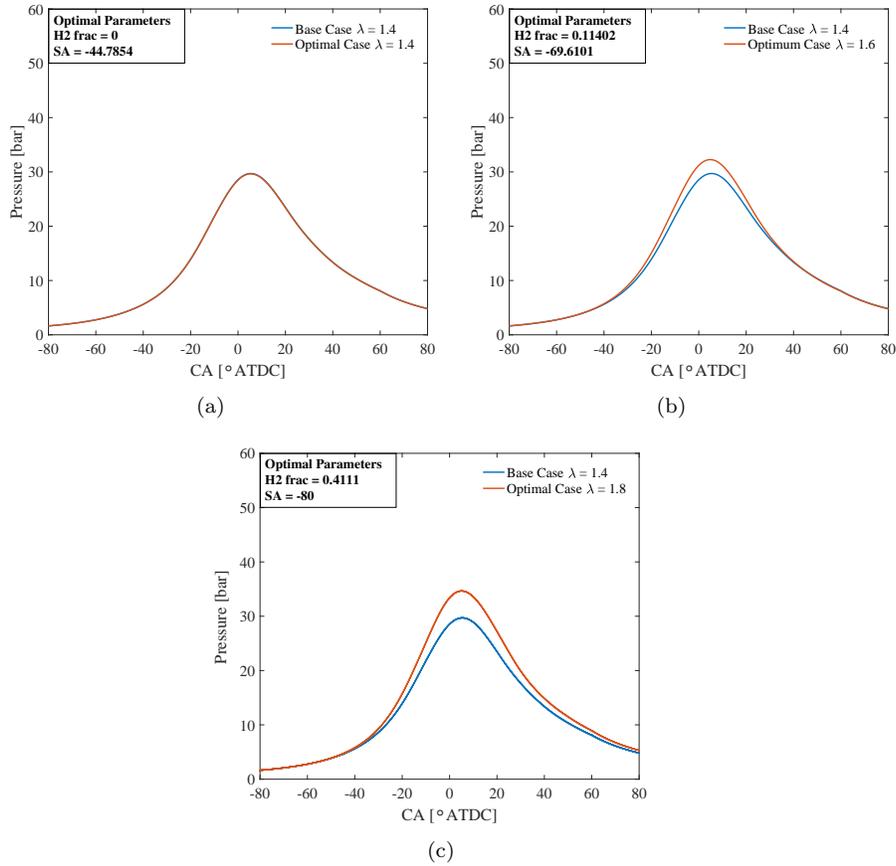
Figure 11: Comparison of in-cylinder pressure evolution for the base and QD-GA optimal methane-hydrogen cases: (a) λ=1.4, (b) λ=1.6, (c) λ=1.8.

temperature associated with ultra-lean mixtures despite syngas addition. Due to the high CO content in the syngas and thereby the low calorific value compared to hydrogen, the in-cylinder combustion temperature and pressure is lower, leading to lower emission levels in the case of methane/syngas blends. The relative amounts of CO and H_2 can have a significant impact on emissions. The thermal and chemical kinetic analyses have shown that the CO content in syngas has a stronger effect on the adiabatic flame temperature, but only plays a minor role in the chemical effect compared to the pure hydrogen addition [59].

The input parameters and the corresponding outputs for both the base case (case 1 in Table 4) and the optimal case from simulations are provided in Table 7. The optimal case found by QD-GA yielded higher indicated thermal efficiencies and reduced NO_x emissions over the base case. Because of the hydrogen content in syngas, its addition to methane increases the flame temperature, which has a

Table 6: Input parameters and outputs for the base and QD-GA optimal methane-hydrogen cases at 3000 rpm.

Parameter	Base case	Optimal case found by the algorithm
Inputs		
Fuel composition (%vol)	100%CH$_4$	58.9%CH$_4$/41.1%H$_2$
Air-fuel ratio (λ)	1.4	1.8
Spark timing (CA BTDC)	45	80
Outputs		
ITE (%)	21.01	31.63
NO$_x$ (ppm)	82.07	13.83

strong effect on NO$_x$ emissions. The increase to of $\lambda = 1.8$ results in significant reduction of the combustion temperature and thus in the NO$_x$ level. It was found that the ultra-lean mixture resulted in reductions of almost 90% of NO$_x$ emissions. Moreover, lower in-cylinder temperatures during the combustion process of ultra-lean mixture led to lower heat losses from the internal elements of the engine and consequently higher thermal efficiencies.

Table 7: Input parameters and outputs for the base and QD-GA optimal methane-syngas cases at 3000 rpm.

Parameter	Base case	Optimal case
Inputs		
Fuel composition (%vol)	100%CH$_4$	50%CH$_4$/50%Syngas
Air-fuel ratio (λ)	1.4	1.8
Spark timing (CA BTDC)	45	80
Outputs		
ITE (%)	21.01	28.52
NO$_x$ (ppm)	82.07	12.03

7. Conclusions

A quasi-dimensional model was employed for the simulation of combustion of a SI engine fueled with methane-hydrogen and methane-syngas fuel blends. The QD model was calibrated and validated against experimental data over a wide range of engine operating conditions and fuel blends. A genetic algorithm approach was implemented and coupled to the quasi-dimensional model to compute the optimal fuel blend and engine input parameters for an SI engine operating with methane/hydrogen and methane/syngas blends. The following key results were found:

- The addition of hydrogen extended methane-fueled SI engines' lean limit operation and enhanced ultra-lean combustion efficiency, achieving both high ITE and low NO$_x$ emissions.

20
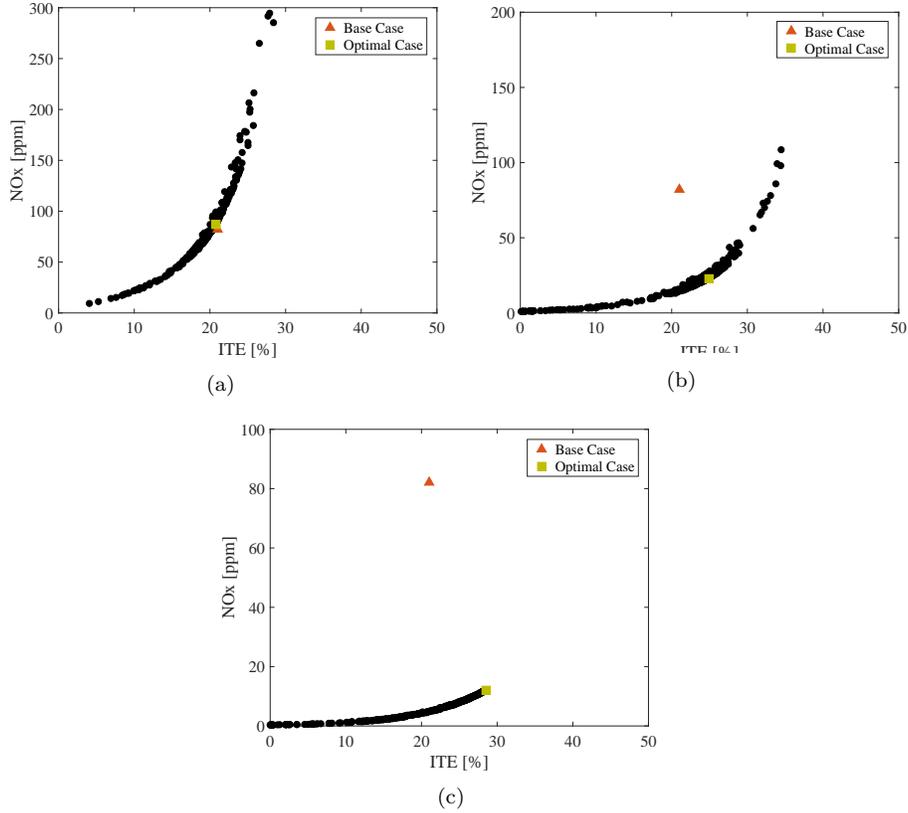
Figure 12: ITE versus NO_x emissions for methane-syngas case including the base and optimum: (a) λ=1.4; (b) λ=1.6; (c) λ=1.8.

- The lean limit extension with higher H_2 fractions of up to about 40% allows for operation at higher λ, where the NO_x-ITE trade-off can be shifted towards NO_x emissions below the base values and higher efficiencies.

- For the methane/hydrogen blends, the optimal blend was found to be 58.9%CH_4/41.1%H_2 at λ=1.8 and spark advance of 80 CAD BTDC. For methane-syngas blends, the optimal blend is 50%CH_4/50%syngas at λ=1.8 and SA of 80 CAD BTDC. It was noticed that the higher hydrogen fraction and λ values are favorable in terms of both efficiency and emissions, where a reduction of engine-out NO_x by 82.5% and a simultaneous increase in ITE by 33.5% were observed.

- Generally, it was found that the present methodology could reach an optimal design with favorable ITE and lower NO_x emissions compared to the pure methane fueled case. The average computational time for one QD-GA simulation case was 44 core-hours compared to the computational fluid
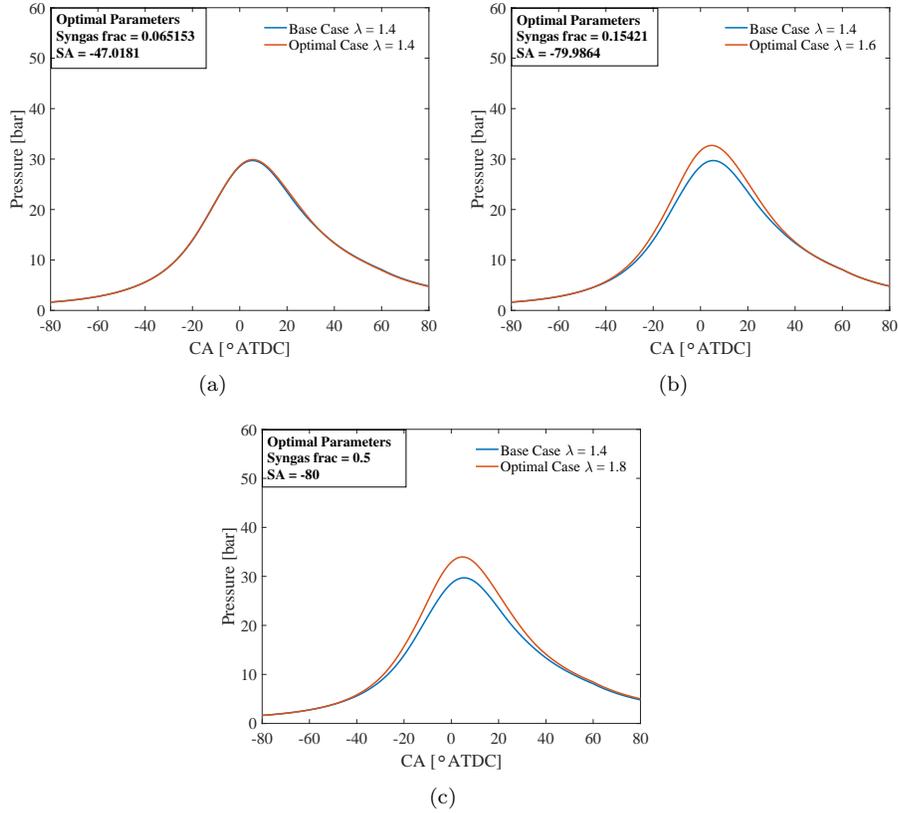
Figure 13: In-cylinder pressure comparison for the base and QD-GA optimal methane-syngas cases: (a) λ=1.4; (b) λ=1.6; (c) λ=1.8.

dynamics (CFD)-GA approach requiring more than 50,000 core-hours for the SI engine simulation [60]. Thereby, this methodology is very efficient and computationally cost-effective as a first screening step.

The methodology can be extended for inclusion of other gaseous fuel blends (e.g. biogas, ethane, propane etc.) and additional engine parameters for future research. In order to perform a comprehensive optimization study, additional operating and design parameters such as compression ratio and EGR could be considered. Currently we are working on the fuel and engine optimization using the CFD-GA approach to determine optimal blends and compare them to the QD-GA results.

Acknowledgements

natural gas engines COST (SBFI/SNF) with number IZCNZ0-174833.

References

[1] T. Korakianitis, A. Namasivayam, R. Crookes, Natural-gas fueled spark-ignition (SI) and compression-ignition (CI) engine performance and emissions, Progress in Energy and Combustion Science 37 (1) (2011) 89–112 (2011).

[2] A.-H. Kakaee, A. Paykani, M. Ghajar, The influence of fuel composition on the combustion and emission characteristics of natural gas fueled engines, Renewable and Sustainable Energy Reviews 38 (2014) 64–78 (2014).

[3] H. M. Cho, B.-Q. He, Spark ignition natural gas engines:A review, Energy Conversion and Management 48 (2) (2007) 608–618 (2007).

[4] F. Ma, S. Ding, Y. Wang, Y. Wang, J. Wang, S. Zhao, Study on combustion behaviors and cycle-by-cycle variations in a turbocharged lean burn natural gas si engine with hydrogen enrichment, International journal of hydrogen energy 33 (23) (2008) 7245–7255 (2008).

[5] A. Sofianopoulos, D. Assanis, S. Mamalis, Effects of hydrogen addition on automotive lean-burn natural gas engines: critical review, Journal of Energy Engineering 142 (2) (2015) E4015010 (2015).

[6] S. O. Akansu, Z. Dulger, N. Kahraman, T. N. Veziroglu, Internal combustion engines fueled by natural gas–hydrogen mixtures, International Journal of Hydrogen Energy 29 (14) (2004) 1527–1539 (2004).

[7] R. K. Mehra, H. Duan, R. Juknelevičius, F. Ma, J. Li, Progress in hydrogen enriched compressed natural gas (HCNG) internal combustion engines-A comprehensive review, Renewable and Sustainable Energy Reviews 80 (2017) 1458–1498 (2017).

[8] A. L. Boehman, O. L. Corre, Combustion of syngas in internal combustion engines, Combustion Science and Technology 180 (6) (2008) 1193–1206 (2008).

[9] P. Rahnama, A. Paykani, V. Bordbar, R. D. Reitz, A numerical study of the effects of reformer gas composition on the combustion and emission characteristics of a natural gas/diesel RCCI engine enriched with reformer gas, Fuel 209 (2017) 742–753 (2017).

[10] L. Tartakovsky, M. Sheintuch, Fuel reforming in internal combustion engines, Progress in Energy and Combustion Science 67 (2018) 88–114 (2018).

[11] Z. Ran, D. Hariharan, B. Lawler, S. Mamalis, Experimental study of lean spark ignition combustion using gasoline, ethanol, natural gas, and syngas, Fuel 235 (2019) 530–537 (2019).

[12] G. Sridhar, P. Paul, H. Mukunda, Biomass derived producer gas as a reciprocating engine fuel?an experimental analysis, Biomass and Bioenergy 21 (1) (2001) 61–72 (2001).

[13] C. A. Rinaldini, G. Allesina, S. Pedrazzi, E. Mattarelli, T. Savioli, N. Morselli, M. Puglia, P. Tartarini, Experimental investigation on a common rail diesel engine partially fuelled by syngas, Energy Conversion and Management 138 (2017) 526–537 (2017).

[14] F. Moreno, M. Muñoz, J. Arroyo, O. Magén, C. Monné, I. Suelves, Efficiency and emissions in a vehicle spark ignition engine fueled with hydrogen and methane blends, International Journal of Hydrogen Energy 37 (15) (2012) 11495–11503 (2012).

[15] G. Kosmadakis, D. Rakopoulos, C. Rakopoulos, Methane/hydrogen fueling a spark-ignition engine for studying NO, CO and HC emissions with a research CFD code, Fuel 185 (2016) 903–915 (2016).

[16] S. Martinez, P. Lacava, P. L. Curto, A. Irimescu, S. S. Merola, Effect of hydrogen enrichment on flame morphology and combustion evolution in a SI engine under lean burn conditions, Tech. rep., SAE Technical Paper (2018).

[17] W. C. Nadaleti, G. Przybyla, B. Vieira, D. Leandro, G. Gadotti, M. Quadro, E. Kunde, L. Correa, R. Andreazza, A. Castro, Efficiency and pollutant emissions of an si engine using biogas-hydrogen fuel blends: BIO60, BIO95, H20BIO60 and H20BIO95, International Journal of Hydrogen Energy 43 (14) (2018) 7190–7200 (2018).

[18] F. Y. Hagos, A. R. A. Aziz, S. A. Sulaiman, R. Mamat, Engine speed and air-fuel ratio effect on the combustion of methane augmented hydrogen rich syngas in di si engine, International Journal of Hydrogen Energy 44 (1) (2019) 477–486 (2019).

[19] A. Paykani, C. E. Frouzakis, K. Boulouchos, Numerical optimization of methane-based fuel blends under engine-relevant conditions using a multi-objective genetic algorithm, Applied Energy 242 (2019) 1712–1724 (2019).

[20] A. Medina, P. L. Curto-Risso, A. C. Hernández, L. Guzmán-Vargas, F. Angulo-Brown, A. K. Sen, Quasi-dimensional simulation of spark ignition engines, Springer, 2014 (2014).

[21] S. Grasreiner, J. Neumann, M. Wensing, C. Hasse, A quasi-dimensional model of the ignition delay for combustion modeling in spark-ignition engines, Journal of Engineering for Gas Turbines and Power 137 (7) (2015) 071502 (2015).

[22] D.-K. Nguyen, L. Sileghem, S. Verhelst, A quasi-dimensional combustion model for spark ignition engines fueled with gasoline–methanol blends, Proceedings of the Institution of Mechanical Engineers, Part D: Journal of Automobile Engineering 232 (1) (2018) 57–74 (2018).

[23] F. Perini, F. Paltrinieri, E. Mattarelli, A quasi-dimensional combustion model for performance and emissions of SI engines running on hydrogen–methane blends, International Journal of Hydrogen Energy 35 (10) (2010) 4687–4701 (2010).

[24] D. Goodwin, H. Moffat, R. Speth, Cantera: An object-oriented software toolkit for chemical kinetics, thermodynamics, and transport processes, version 2.3. 0, 2017, doi: 10.5281/zenodo. 170284http, URL http://www. cantera. org.

[25] H. Lee, A. Mohamad, L. Jiang, A detailed chemical kinetics for the combustion of H2/CO/CH4/CO2 fuel mixtures, Fuel 193 (2017) 294–307 (2017).

[26] W. K. Metcalfe, S. M. Burke, S. S. Ahmed, H. J. Curran, A hierarchical and comparative kinetic modeling study of C1- C2 hydrocarbon and oxygenated fuels, International Journal of Chemical Kinetics 45 (10) (2013) 638–675 (2013).

[27] M. Van Essen, S. Gersen, G. Van Dijk, H. Levinsky, Two-zone thermodynamic model to predict temporal variations in pressure of the end gas in an engine cylinder cycle, Tech. rep., SAE Technical Paper (2013).

[28] M. S. Lounici, K. Loubar, M. Balistrou, M. Tazerout, Investigation on heat transfer evaluation for a more efficient two-zone combustion model in the case of natural gas SI engines, Applied Thermal Engineering 31 (2-3) (2011) 319–328 (2011).

[29] S. Verhelst, C. Sheppard, Multi-zone thermodynamic modelling of spark-ignition engine combustion–an overview, Energy Conversion and Management 50 (5) (2009) 1326–1335 (2009).

[30] C. Rakopoulos, C. Michos, E. Giakoumis, Thermodynamic analysis of SI engine operation on variable composition biogas-hydrogen blends using a quasi-dimensional, multi-zone combustion model, SAE International Journal of Engines 2 (1) (2009) 880–910 (2009).

[31] S. Hann, L. Urban, M. Grill, M. Bargende, Prediction of burn rate, knocking and cycle-to-cycle variations of binary compressed natural gas substitutes in consideration of reaction kinetics influences, International Journal of Engine Research 19 (1) (2018) 21–32 (2018).

[32] N. C. Blizard, J. C. Keck, Experimental and theoretical investigation of turbulent burning model for internal combustion engines, Tech. rep., SAE Technical Paper (1974).

[33] R. D. Matthews, M. J. Hall, W. Dai, W. Dai, G. C. Davis, Combustion modeling in SI engines with a peninsula-fractal combustion model, SAE Transactions (1996) 180–195 (1996).

[34] C. Ji, J. Yang, X. Liu, B. Zhang, S. Wang, B. Gao, A quasi-dimensional model for combustion performance prediction of an SI hydrogen-enriched methanol engine, International Journal of Hydrogen Energy 41 (39) (2016) 17676–17686 (2016).

[35] J. Pashaei, R. K. Saray, Development of a quasi-dimensional, fractal-base combustion model for SI engines by simulating flame-wall interaction phenomenon, Fuel 236 (2019) 13–29 (2019).

[36] V. De Bellis, F. Bozza, D. Tufano, A comparison between two phenomenological combustion models applied to different SI engines, Tech. rep., SAE Technical Paper (2017).

[37] F. Bozza, A. Gimelli, S. S. Merola, B. Vaglieco, Validation of a fractal combustion model through flame imaging, Tech. rep., SAE Technical Paper (2005).

[38] R. D. Matthews, Y.-W. Chin, A fractal-based SI engine model: comparisons of predictions with experimental data, SAE Transactions (1991) 99–117 (1991).

[39] S. Chung, C. Law, An integral analysis of the structure and propagation of stretched premixed flames, Combustion and Flame 72 (3) (1988) 325–336 (1988).

[40] D. A. Santavicca, D. Liou, G. L. North, A fractal model of turbulent flame kernel growth, SAE Transactions (1990) 90–98 (1990).

[41] M. J. Hall, F. Bracco, A study of velocities and turbulence intensities measured in firing and motored engines, SAE Transactions (1987) 414–441 (1987).

[42] A. Lipatnikov, J. Chomiak, Turbulent flame speed and thickness: phenomenology, evaluation, and application in multi-dimensional simulations, Progress in Energy and Combustion Science 28 (1) (2002) 1–74 (2002).

[43] G. F. Hohenberg, Advanced approaches for heat transfer calculations, Tech. rep., SAE Technical paper (1979).

[44] D. N. Assanis, J. B. Heywood, Development and use of a computer simulation of the turbocompounded diesel system for engine performance and component heat transfer studies, SAE Transactions (1986) 451–476 (1986).

[45] X. Zhen, Y. Wang, S. Xu, Y. Zhu, C. Tao, T. Xu, M. Song, The engine knock analysis–an overview, Applied Energy 92 (2012) 628–636 (2012).

[46] Z. Wang, H. Liu, R. D. Reitz, Knocking combustion in spark-ignition engines, Progress in Energy and Combustion Science 61 (2017) 78–112 (2017).

[47] L. Chen, T. Li, T. Yin, B. Zheng, A predictive model for knock onset in spark-ignition engines with cooled EGR, Energy Conversion and Management 87 (2014) 946–955 (2014).

[48] K. F. H. M. Steurs, Cycle-resolved analysis and modeling of knock in a homogeneous charge spark ignition engine fueled by ethanol and iso-octane, Ph.D. thesis, ETH Zurich (2014).

[49] F. Bozza, V. De Bellis, L. Teodosio, A tabulated-chemistry approach applied to a quasi-dimensional combustion model for a fast and accurate knock prediction in spark-ignition engines, Tech. rep., SAE Technical Paper (2019).

[50] J. Livengood, P. Wu, Correlation of autoignition phenomena in internal combustion engines and rapid compression machines, in: Symposium (international) on combustion, Vol. 5, Elsevier, 1955, pp. 347–356 (1955).

[51] A. Douaud, P. Eyzat, Four-octane-number method for predicting the anti-knock behavior of fuels and engines, SAE Transactions (1978) 294–308 (1978).

[52] J. B. Heywood, et al., Internal combustion engine fundamentals (1988).

[53] F. Ma, Y. Wang, H. Liu, Y. Li, J. Wang, S. Zhao, Experimental study on thermal efficiency and emission characteristics of a lean burn hydrogen enriched natural gas engine, International Journal of Hydrogen Energy 32 (18) (2007) 5067–5075 (2007).

[54] D. T. Montgomery, An investigation into optimization of a heavy-duty diesel engine operating parameters when using multiple injections and EGR, Ph.D. Thesis, University of Wisconsin-Madison (2000).

[55] S. Gersen, M. van Essen, G. van Dijk, H. Levinsky, Physicochemical effects of varying fuel composition on knock characteristics of natural gas mixtures, Combustion and Flame 161 (10) (2014) 2729–2737 (2014).

[56] J. Huang, W. Bushe, P. Hill, S. Munshi, Experimental and kinetic study of shock initiated ignition in homogeneous methane–hydrogen–air mixtures at engine-relevant conditions, International Journal of Chemical Kinetics 38 (4) (2006) 221–233 (2006).

[57] S. Gersen, N. Anikin, A. Mokhov, H. Levinsky, Ignition properties of methane/hydrogen mixtures in a rapid compression machine, International Journal of Hydrogen Energy 33 (7) (2008) 1957–1964 (2008).

[58] Z. He, Z. Gao, L. Zhu, S. Li, A. Li, W. Zhang, Z. Huang, Effects of H_2 and CO enrichment on the combustion, emission and performance characteristics of spark ignition natural gas engine, Fuel 183 (2016) 230–237 (2016).

[59] Q. Zhou, C. Cheung, C. Leung, X. Li, X. Li, Z. Huang, Effects of fuel composition and initial pressure on laminar flame speed of $H_2/CO/CH_4$ bio-syngas, Fuel 238 (2019) 149–158 (2019).

[60] A. A. Moiz, P. Pal, D. Probst, Y. Pei, Y. Zhang, S. Som, J. Kodavasal, A machine learning-genetic algorithm (ML-GA) approach for rapid optimization using high-performance computing, SAE International Journal of Commercial Vehicles 11 (2018-01-0190) (2018) 291–306 (2018).

28